Input gain control confers robust combinatorial odor coding in naturalistic environments

Nirag Kadakia[1,2] and Thierry Emonet[2,3]

[1] Swartz Fellow of Theoretical Neuroscience
[2] Department of Molecular, Cellular, and Developmental Biology, Yale University, New Haven, CT 06511, USA
[3] Department of Physics, Yale University, New Haven, CT 06511, USA

February 27, 2018

Animals can identify and discriminate a myriad of odors using a surprisingly limited class of distinct olfactory receptor genes. It was recently noted that a critical feature of our odor environment may resolve this inconsistency: most naturally-occurring odors are composed of only a tiny subset of these many volatile molecular constituents [1]. In principle, the high-dimensional odor signal could be accurately decompressed from a limited number of receptor measurements, provided (i) the odor signal is sufficiently sparse in odorant space and (ii) the responses are sufficiently dispersed. The latter requires that odor receptors bind many odorants with distinct affinities, and that a given odorant elicits responses in several such receptors. Odor identity is therefore coded in the unique combination of responses the odor elicits in the sensing repertoire. Indeed, it has been found that many olfactory receptor neurons (ORNs) in the sensing peripheries of fruit flies [2] and mosquitos [3] exhibit such a dispersed response to a large panel odorants, suggesting that odor identities are encoded combinatorially in unique patterns of response.

In *Drosophila melanogaster*, transformations of ORN activity in the subsequent neural circuitry lend further credence to this combinatorial coding strategy. ORNs housed in the sensing hairs (sensilla) of the antenna synapse to neuropil compartments in the antennal lobe called glomeruli (ORNs expressing a given Or synapse to the same glomerulus), where they then divergently and randomly synapse to Kenyon cells in the mushroom body (MB) and lateral horn (LH) [4, 5]. In the MB, the responses are decoded and sent to higher order brain centers where they are translated to behavioral response [6, 7]. As has recently been argued, the expansive synaptic connections from AL to MB [5] may play a key role in learning and robust odor discrimination in this coding framework [1].

As combinatorial coding relies fundamentally on a dispersed response, a potential complication is response saturation. Maximum ORN firing rates increase with single odorant concentration rather inhomogenously, potentially jeopardizing response breadth as odor concentrations change. For example, ORNs expressing the receptor Or35a initially fire at varying rates spanning 30 to 300 Hz, in response to half-second puffs of one of eleven distinct odorants at dilutions of 10^{-4} [2]. But at dilutions of 10^{-2}, these maximum firing rates have all elevated to a narrow range between 200 and 250 Hz. Similar apparent saturation occurs for ORNs expressing Or85b, Or22a, and OR67a in response to the same panel of odorants. Since such wide fluctuations in odor concentrations are not atypical in natural environments [8], it is unclear how sensitivity could be maintained if ORN responses were to saturate so easily.

On the other hand, it has been shown that *Drosophila* ORN local field potentials and firing rates adapt to odor stimuli in time [9, 10, 11]. In particular, in response to a fluctuating monomolecular signal, firing rate gain scales inversely with mean odor concentration, according to the Weber-Fechner law observed in vision [11, 12, 10]. This rapid adaptation has been traced back to molecular mechanisms operating at the level of odor transduction, upstream of ORN firing machinery [10]. Importantly, this observed scaling law was obeyed by several combinations of ORNs and odorants, pointing to a mechanistic origin involving the universal co-receptor Orco [13]. Further implicating Orco in gain modulation, though over longer timescales, is the observation that Orco dephosphorylizes following prolonged exposure to odors, leading to receptor desensitization [14, 15]. Finally, in addition to front-end adaptation, normalization enacted through lateral inhibition in the AL may act as a mechanism of gain control further downstream [16].

While all of these adaptive mechanisms have been shown to facilitate the identification of temporally varying monomolecular odorants, we know little about their potential role in odor discrimination. To address this question, we combined a biophysical model of dispersed odor binding, ORN activation, and adaptive gain control in the *Drosophila* olfactory periphery with a neural framework for decoding distributed ORN responses. We find that front-end adaptation enacted through the Weber-Fechner Law aids the accurate identification of complex odors and the discrimination of conflicting odor signals across wide variations in odor intensity. Further, we find that this adaptive mechanism promotes the discrimination of odor signals in dynamic odor landscapes and amid fluctuating odor backgrounds. Together, our findings suggest a fundamental role for input gain control in maintaining olfactory sensitivity within naturalistic odor environments.

Results

a A model of odor encoding that preserves the diversity of ORN response and adaptive scaling

The framework of odor discrimination consists of two stages: odor transduction and subsequent ORN activity (encoding), and a paradigm for then inferring odor identity from this repertoire of ORN response (decoding). The encoding model is a generalization of one recently used to describe front-end adaptation in individual *Drosophila* ORNs [10]. Here, we generalize this model to a repertoire of a ORNs, each housing a collection of Or/Orco complexes. These complexes bind and unbind odorant molecules stochastically, and are assumed to reside in either an active (open ion channel) or inactive state. In equilibrium, a given odorant-receptor pair (i-a) depends on two disassociation constants, K^*_{ia} and K_{ia}, for odorant binding in the active and inactive conformations, respectively. Together, these comprise a coupled stochastic system that translates the binding of odors of varying identities and concentrations into a repertoire of ORN response (Fig. 1a). In steady state, the active fraction A_a of Or/Orco complexes in ORN a is:

$$A_a = \left(1 + e^{\epsilon_a} \frac{1 + \sum_i^N s_i/K_{ia}}{1 + \sum_i^N s_i/K^*_{ia}}\right)^{-1}, \qquad (1)$$

where s_i is the concentration of the odorant i and ϵ_a is the free energy of activation for a particular Or/Orco complex. Weber's Law can be satisfied by scaling ϵ_a with the average odorant concentration, $\epsilon_a \sim \ln\langle s_i\rangle$.

Ignoring for the moment the slower effects of adaptation (i.e., assuming ϵ_a is fixed), this model represents the instantaneous change in the activity as a function of ligand concentration, i.e. similar to the maximum firing rate measured in [2]. We first show that the steady state response reproduce the diversity of observed ORN tuning curves. Olfactory receptors in *Drosophila* can range from narrowly tuned, responding to a single odorant, to quite broad, responding to various distinct odorants spanning multiple functional groups. We incorporate this diversity of response into our framework by treating K^*_{ia} and K_{ia} as random variables with pre-defined statistics. Figures 1b-1d shows how a simple choice of statistics on $K^*_{i,a}$ can naturally produce a diverse repertoire of response closely mimicking observed *Drosophila* ORN tuning curves.

By enforcing Weber's Law, we can maintain this distributed response across concentration changes (Fig. 1e). Fig. 1f shows the response of three ORNs to distinct complex but sparse odors at varying mean odor concentrations. Without adaptive feedback, the breadth of the firing rate distributions narrow, homogenizing the responses across odor identity. If the ORN repertoire produces the same pattern of activity in response to distinct odors, odor identity information is lost. Conversely, by scaling $\epsilon_a \sim \ln\langle s_i\rangle$, distributed responses are maintained through a large range of concentrations. As we will see, the maintenance of this disperse response is central to reliable odor decoding in fluctuating environments.

b Adaptive feedback preserves identity and intensity in sparse decoding

In *Drosophila*, odorant identity is inferred from spatiotemporal patterns of neural activity in Kenyon cells housed in the mushroom body. Since these activity patterns result from a combination of ORN response and downstream neural processing, front-end gain control can play a crucial role in preserving neural representations of odor identity. The complicating factor in signal reconstruction is the disparity between measurement dimension and stimulus dimension: while *Drosophila* only express 60 olfactory receptor genes, the space of aromatic odorants is 10^3 or more, suggesting that decoding is a fundamentally under-determined problem. However, as noted, naturally-occurring odors are comprised of only a small subset of these volatile compounds – they are sparse in the space of odorants [1]. This is suggestive as mathematical results in the theory of compressed sensing guarantee the reconstruction of these sparse signals, assuming a sufficiently random response [17, 18, 19].

Of course, large fluctuations in intensity characteristic of naturalistic environments could markedly affect response combinatorics or quench activity dispersedness (as in Fig. 1f), limiting decoding fidelity. Conversely, we expect that since imposing the Weber-Fechner scaling relation maintains the receptor activity distribution over the dynamic range of ϵ_a, odor representations can be preserved naturally amid concentration changes.

To incorporate the linear framework of compressed sensing into our nonlinear encoding model, we treat the odor encoding process exactly, while approximating the decoding to first order. Specifically, we represent the nonzero components s_k of the sparse odor signal as $s_k = s_0 + \Delta s_k$, where s_0 is the center of the linearization. The target of the decoding process

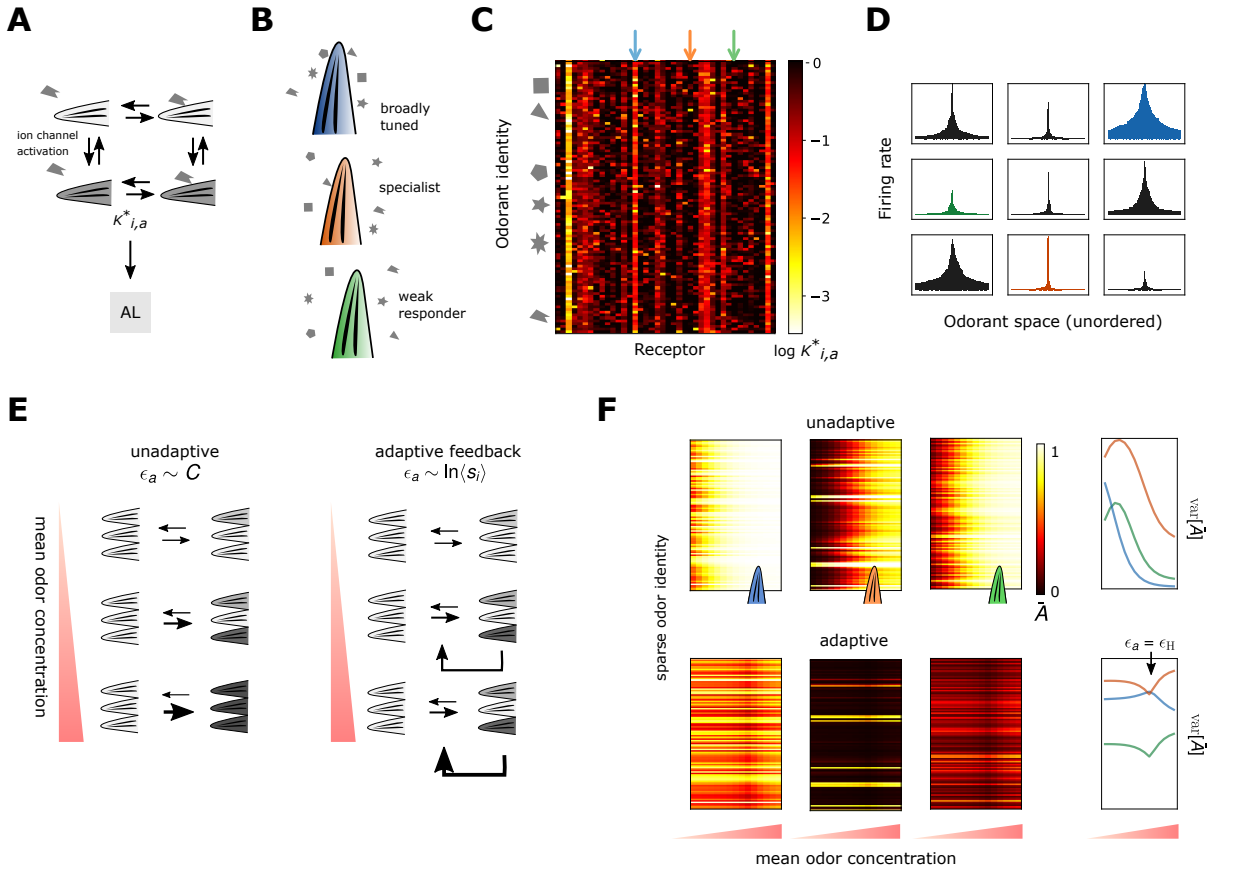

Figure 1: **A** Odor binding model. Odorants bind to Or/Orco complexes, which may be quiescent (light gray) or active (dark gray). The likelihood that a complex is in an active state depends on its binding affinity to constituent odor molecules (through $K^*_{i,a}$) and the energetic cost of receptor activation. **B** Or classes exhibit distinct binding distributions. **C** Example instantiation of the active binding disassociation matrix $K^*_{i,a}$ (see Methods). **D** Sample Or/Orco activity of 9 of the 40 ORNs represented by the matrix in (C). The tuning curves, individually ordered by odorant for visualization, exhibit broad, specialized, and weak responses. **E** Schematic of Weber Law feedback at signal transduction. When Weber Law is enforced, activity distributions of active complexes (shaded darkly) remain invariant with increasing signal concentrations. **F** Steady state Or/Orco activity for the three sample ORNs in (B), (C), and (D), in an unadaptive system (top row) and adaptive system (bottom row) in response to 100 different sparse odors; each matrix row corresponds to a distinct odor identity. The variance of Or/Orco activity across odor identity can rapidly diminish in the absence of front-end adaptation (final column).

are the identities and intensities of the 'excess' signals Δs_i. To assess the decoding performance, we denote an odor signal as accurately decoded if (i) the sparse odorant components are all estimated to within 25% of their correct value and (ii) the components absent in the original signal ("zero" components) are all estimated as less than 10% of the mean excess concentration, $\hat{s}_j \leq \langle \Delta s_k \rangle$. The former is a measure of accurately inferring signal *intensity*; the latter of signal *identity*.

We apply this scheme to receptor systems consisting of 50 Or/Orco complexes interacting with a 100-dimensional odorant space. Without adaptive feedback, nearly all 100 random sparse odor signals (each odor has 7 nonzero odorants) are still correctly inferred in a particular regime of mean odor concentration (Figs. 2a and 2b; blue curves). We find that this holds true for two distinct neural systems, one of which contains homogeneously but all broadly responding receptors (for each a, K^*_{ia} are sampled from the same distribution), the second of which is more indicative of *Drosophila* physiology and exhibits a diverse repertoire ranging from broad to highly specialized (as in Fig. 1). In both cases, however, decod-

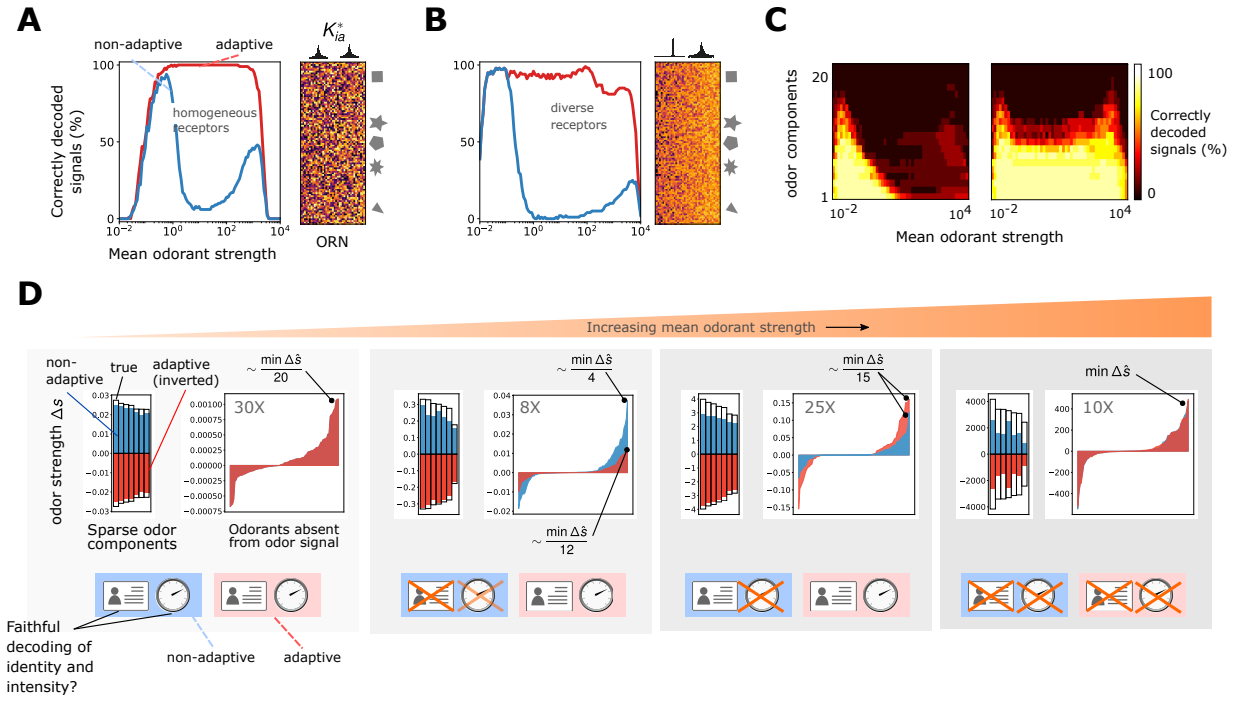

Figure 2: Input adaptation aids robust odor signal reconstruction through a wide range of odor concentration changes. **A** Percent correctly decoded odors, with (red) and without (blue) Weber Law adaptation, for a homogeneous system in which the binding statistics of each receptor are chosen from the same distribution. The heatmap of the K^*_{ia} matrix illustrates receptor homogeneity. **B** Same as (A), but now for a diverse receptor repertoire more indicative of *Drosophila* physiology. **C** Dependence of decoding accuracy on odor sparsity. At low concentrations, both systems can decode relatively complex signals; as concentration increases, complex signals are mis-identified in the absence of adaptive feedback. **D** Separation of intensity and identity decoding. At low concentrations, both signal identity and intensity are correctly inferred in a non-adaptive system. Increases in signal concentrations can lead to errors in odor intensity, identity, or both. When Weber Law is enforced, the representation of odor intensity and its identity are maintained through a wide regime of odor concentrations.

ing fidelity is not concentration invariant, dropping sharply outside this regime of faithful signal decoding.

Conversely, we hypothesize that by stabilizing the excess activity levels through Weber-Fechner adaptive feedback, such sensitivity can be mitigated. Enforcing this scaling law above a mean odor concentration of $s_0 = 10^{-1}$, and matching ϵ_a to the unadaptive system otherwise, we find that coding fidelity is now maintained over a five-fold change (a.u.) in odor concentration (Fig. 2a; red curves). This invariance holds across differing levels of signal sparsity (Fig. 2c). In the adaptive system, signals with complexity as high as 10 odorants are robustly decoded over several orders of odor concentration. In the non-adaptive system even mono-molecular signals are mis-identified at increased concentrations, a consequence of response homogenization across the ORN repertoire.

A critical feature of olfactory systems is the ability to simultaneously decode odor intensity and identity, aspects which can in principle overlap [20, 21]. Compressed decoding conflates these two aspects into a single computation by inferring not only the exact component magnitudes of an odor signal (intensity), but also which molecular components constitute the high-dimensional signal in the first place (identity). Despite the conflation of these in practice, it is possible that in this framework, one aspect may be preserved while the other is violated.

Separating errors in odor intensity from those in error identity, we find that for an un-adaptive system, either or both may contribute depending on odor concentration. For moderate concentrations, the inferred zero components reach a substantial fraction of the mean odor concentration, while the estimates

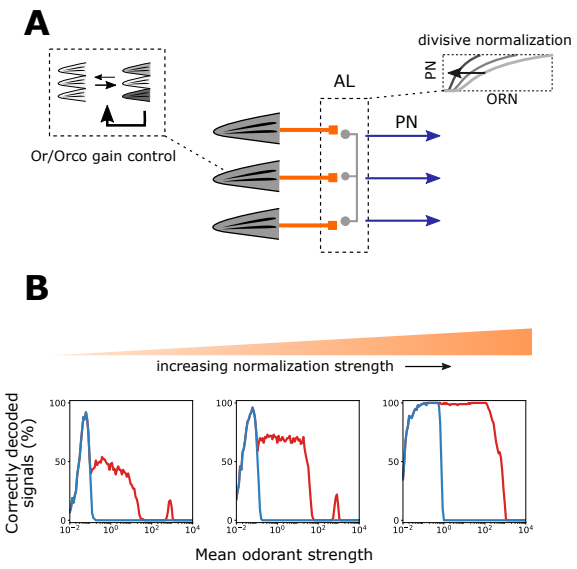

Figure 3: **A** Schematic of divisive normalization / lateral inhibition B Increasing divisive normalization w and w/o Weber Law

of the sparse components are largely even with their true values – the identity of the odor is compromised (Fig. 2d). As concentrations increase further, identity is now preserved (zero components are estimated well below the mean), but errors in odor intensity have magnified. This illustrates that in the absence of front-end gain control, errors both in identity and intensity can confound odor representations, while Weber Law feedback can mitigate these conflicts.

c Inhibitory normalization

forthcoming; perhaps put this in previous section and relegate figures to SI?

d Weber Law scaling aids odor discrimination in conflicting environments

Olfactory sensing in naturalistic settings relies on the ability to discriminate multiple odors, which may differ or overlap in chemical makeup and intensity. Though Weber Law adaptation can preserve decoding accuracy over changes in odor intensity, a system which adapts to mean concentrations alone may well fail in the presence of distinct odors of differing concentrations. To test this, we consider two sparse odors. The first we call the "foreground" odor, and hold its component concentrations fixed at $s_{k,\mathrm{F}}$. The second, which can span intensities a few orders below or above $s_{k,\mathrm{F}}$, we refer to as the "background" odor, investigating how its intensity and complexity can affect the identification of the foreground signal. We maintain the total nonzero components of the signal at 7, but split these seven components between the two odors in increasing ratios.

We first find that molecularly complex backgrounds, if sufficiently strong, can confuse the identification of single odorant foregrounds, both for adaptive and non-adaptive systems (Fig. 4a). Still, the adaptive case is more robust to decoding errors, maintaining accuracy to a higher concentration. Meanwhile, the background odor is now misidentified in the non-adaptive system, until its concentration has sufficiently surpassed the simpler foreground (Fig. 4e). Importantly, there is no regime in which both odors are correctly identified by a non-adaptive system. Conversely, enforcing Weber's Law robustly identifies both odors in a window of concentrations between 0.1 to 1 (a.u.).

When the foreground odor consists of more molecular constituents (but is still less complex than the background), it is more robustly decoded in a non-adaptive system (Fig. 4d); however, the foreground signal is more commonly mis-estimated (Fig. 4c). This pattern continues as the complexity of the odors are about equal (Fig. 4e and Fig. 4f). Meanwhile, the accuracy of the adaptive system remains relatively robust, and its window of accurate odor discrimination has increased. Finally, we find that odors are most easily discerned amid backgrounds of varying concentrations when these backgrounds are molecularly simple (Fig. 4g and 4h). While a window of faithful odor discrimination has appeared in the non-adaptive system, this regime is markedly larger in the adaptive case.

Together, these results show that in some cases a non-adaptive system of distributed receptors can still discriminate two odors of differing concentrations, but accuracy is sensitive to odor complexity. Conversely, by adapting receptor gain to the mean odor concentration in accordance with Weber's Law, discrimination accuracy is robustly maintained over a large range of odor concentrations and relative molecular complexities. This suggests that a non-specific strategy of adapting receptor sensitivity to average ORN activity, irrespective of odor identity, can promote accurate odor discrimination in conflicting odor

environments.

e Dynamic adaptation preserves active odor perception in fluctuating odor environments

So far, we have assumed that odor signals are static in time, and that adaptation from the neural circuitry feeds back onto the receptor sensitivity instantly and perfectly. But realistic odor environments are highly intermittent and widely fluctuating, exhibiting odor concentrations that can span several orders [8]. Further, limitations on energy consumption can limit adaptation speed and accuracy [22]. To account for temporal aspects in both the odor environment and sensing periphery, we relax the assumption that adaptation is instantaneous, instead letting the activity of each Or/Orco complex decay linearly to baseline levels $\bar{A}_a$ via accompanying modulation of the complex free energies. Specifically, in response to a dynamic odor signal $s(t)$, the activity of complex a is still given by Eq. 1, but now with time-dependent free energies, $\epsilon_a \to \epsilon_a(t)$ obeying the dynamics

$$\frac{d\epsilon_a(t)}{dt} = \frac{1}{\tau_a}\left[A_a - \bar{A}_a\right], \tag{2}$$

where $A_a = A(s(t), \epsilon_a(t))$ is the time-dependent activity level and τ_a sets the timescale of adaptation. We compare the results for several timescales between 10 ms and several seconds. In accordance with out assumption that the adaptive mechanism acts on the universal co-receptor Orco, we assume that the adaptation timescale is receptor-independent, $\tau_a \equiv \tau$.

To mimic a naturalistic odor signal, we used recorded traces from a photo-ionization detector whose statistics were verified to match those of natural odor plumes (Fig. 5a) [8]. The signals was scaled to values applicable to our model framework (in arbitrary units).

Considering first a set of 20 randomly chosen sparse odors of unique identities, we plot in Fig. 5b decoding errors arising from either mis-identification of odor identity, or that of odor intensity, in two windows containing odor whiffs. For slow adaptation, with timescales greater than a few hundred ms (lighter curves in Fig. 5b), we find clear trends in both intensity and identity coding. Errors in odor intensity are quite sensitive to the faster fluctuations in the odor signal, even if the signal remains appreciable throughout the whiff. While 80% of the odorant identity is perceived immediately at whiff threshold, the estimate accuracy fails to improve from then onward through the duration of the whiff. Conversely, with faster adaptation ($\tau < 100$ ms), the coding of odor intensity corrects within the first 100 ms of the whiff onset (dark red curves). Interestingly, odor intensity coding improves steadily as the whiff endures, though it takes several times the adaptation timescale to minimize the errors.

To illustrate this in more detail, we consider the errors for only one of the 20 sparse signals, at the onset and closure of the whiff demarcated by the purple and blue markers in Fig. 5a and 5b. In Fig. 5c, we plot estimates of the nonzero components of the sparse odor signal at whiff onset and whiff closure for the timescales $\tau = 460$, 180, and 78. For higher adaptation rates, there is some improvement in the estimate of odor intensity by the end of the whiff, but the gains are rather small. On the other hand, the perception of odor identity is particularly frustrated by slow adaptation. For $\tau = 460$, the fraction of zero odor components perceived at >10% of the mean odor signal $\langle \Delta s_k \rangle$ is substantial at whiff onset, and remains unchanged by the end of the whiff (Fig. 5d). For $\tau = 78$, the mis-estimated proportion is equivalent at whiff onset, but has vanished by whiff end. This is further corroborated by averaging over all whiffs (Fig. 5e). Together, this illustrates that dynamic front-end adaptation to mean signal intensity actively aids the perception of odor identity in intermittent odor environments.

Finally we ask: Can adaptive feedback can actively improve the the perception of odor identity in the presence of dynamic adaptation, fluctuating odors *and* fluctuating backgrounds? We consider three cases, in which a background odor modulates on timescales roughly that of the foreground, somewhat slower, and substantially slower. To maximize potential conflicts, we assume the foreground and background odors span odor intensities of roughly equal magnitude. In addition, anticipating our earlier results (Fig. 4), we consider various levels of relative complexity among these two odors.

When the timescale of background fluctuations is long, we find that performance improves markedly with adaptation speed (mis-identified zero components drop from 14 to 0 as timescale varies from 10 seconds to 0.5 seconds), but is already maximized at 500 ms, which exceeds the duration of most of the odor whiffs. In other words, contrary to the single odor case, odors are perfectly identified even when adaptive gain operates at timescales somewhat slower

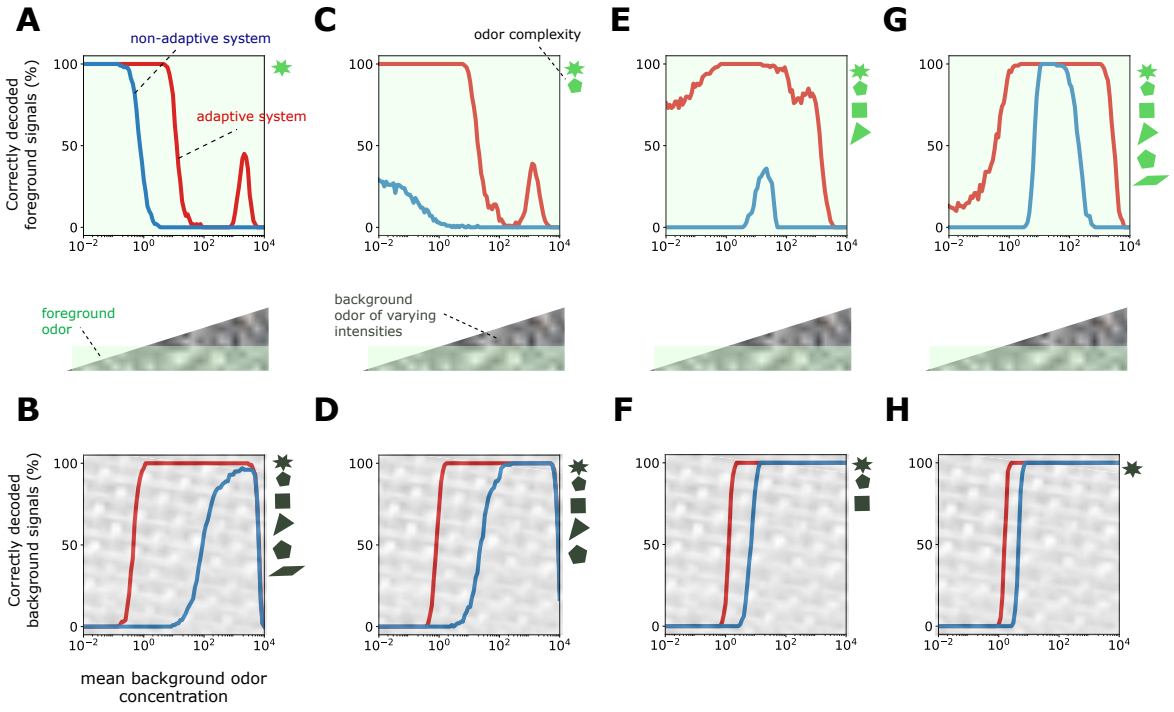

Figure 4: Input adaptation promotes discrimination of distinct odors across conflicts in molecular complexity. **A/B** Percentage of correctly decoded sparse odor signals with 7 nonzero components, each consisting of a 1-component foreground odor at a concentration of $s_{k,\mathrm{F}} \sim 1$ and a 6-component background odor, as a function of background odor intensity. The estimate for the foreground odor components are shown in (A); the background components in (B), averaged over 100 odor identities; non-adaptive system plotted in blue and adapting system in red. **C-H** Corresponding plots for foreground/background component ratios of 2:5, 4:3, and 6:1.

than the signal fluctuations. For slightly faster background fluctuations, but still slower than the foreground timescale, we see a marked degradation in performance with slower adaptation, although again the performance largely saturates at timescales of 500 ms or so. Further, there is now a strong dependence on foreground complexity; simpler foregrounds are easier to perceive above the background (number of mis-identified zero components $\sim$ 3), while very complex foregrounds have a larger number of misidentified components $\sim$ 8. This pattern continues when the background fluctuates as quickly as the foreground, though the performance is only slightly degraded. Importantly, there is a monotonic gain in performance as adaptation speed increases, holding across fluctuation timescales and molecular complexity. Our key finding is that for odors that fluctuate on well-separated timescales, dynamic adaptive feedback obeying the Weber-Fechner Law and operating moderately quickly promotes the active perception of odor identity.

Discussion

Drawing on recent evidence for the existence of the Weber-Fechner law in in *Drosophila* olfactory receptor neurons [12, 11, 10], we propose a theoretical framework for the adaptive encoding and decoding of complex, dynamic odor environments. We argue that this adaptive mechanism, when incorporated into a combinatorial coding strategy, is central to the accurate identification and discrimination of rapidly fluctuating, potentially conflicting odor signals. Our framework relies on two steps of odor encoding and decoding, respectively: (i) a nonlinear, stochastic model of odor-receptor binding and subsequent receptor activity, and ii) reconstruction of the signal via compressed decoding of the neural response. In this

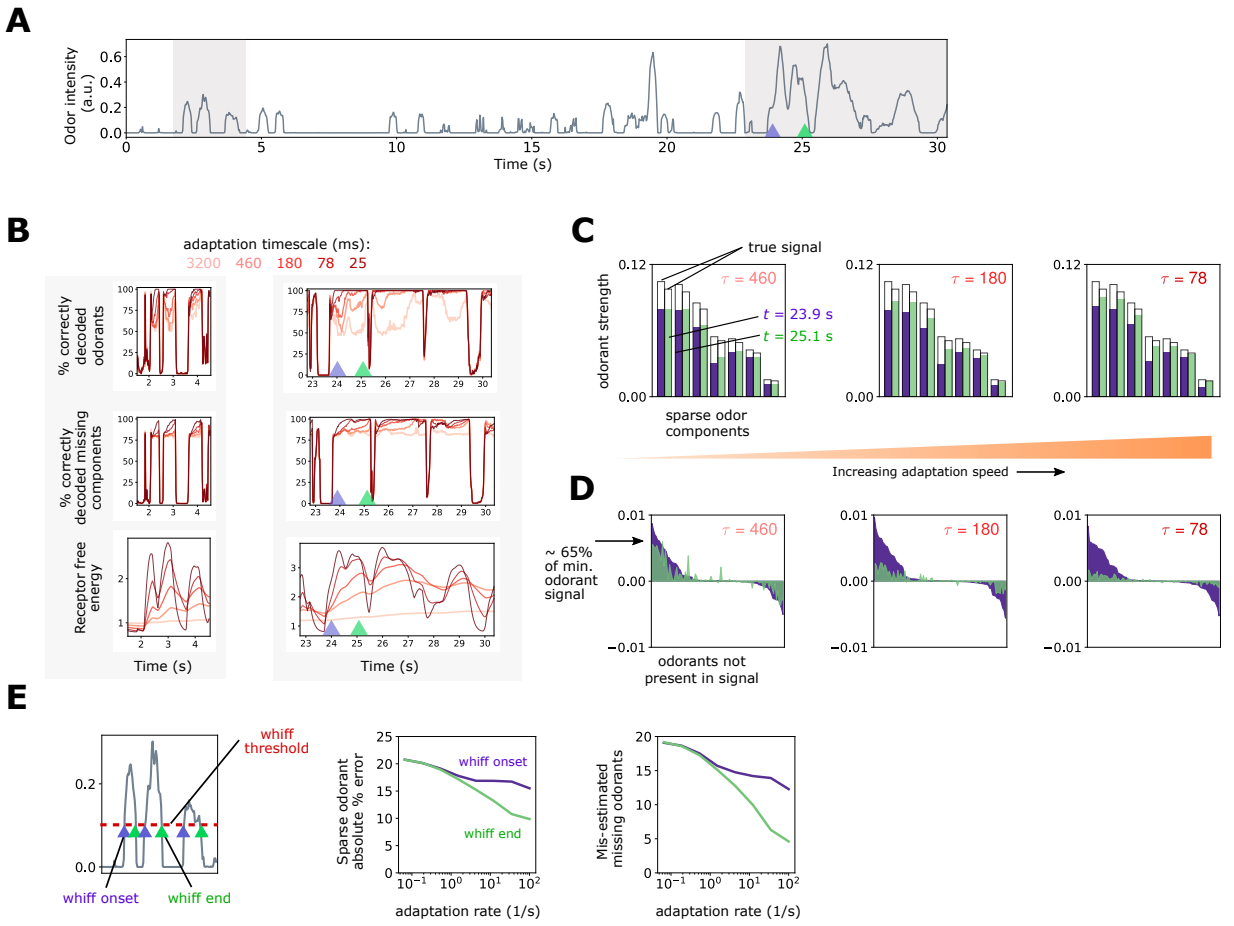

Figure 5: Dynamic front-end adaptation aids active perception of odor identity in naturalistic odor environments. **A** Time course of mean odor signal concentration s_0. **B** By row, percentage of correctly decoded nonzero components of sparse odors, percentage of correctly decoded zero components, and receptor activation energies ϵ_a, throughout the time course of two shaded regions in (A), for adaptation timescales range from long (light red) to short (dark red). Percentages are determined by averaging over 20 distinct estimated odor identities. **C** Estimates of the sparse components of one of the 20 odor identities at the beginning and end of the whiff denoted by the purple and green markers in (A) and (B), for different adaptation timescales. **D** Estimates of zero components of the odor signal corresponding to the same whiff, odor identity, and timescales as in (C). Odor components (which should be zero) are ordered by magnitude of estimate at whiff onset (purple); some components are mis-estimated to be as high as 2/3 of the smallest component of the sparse odor. **E** Errors in sparse and zero components of odor signals as a function of adaptation rate, averaged over all 20 odor identities and all whiff encounters, determined by a threshold concentration of 0.1 (a.u.)

framework, input gain control following the Weber-Fechner Law is enforced by appropriate scaling of the free energy of Or/Orco complex activation with the odor signal mean.

The encoding model is a generalization of the classical model of bacterial chemotaxis [23], and is mathematically equivalent to a recently proposed competitive binding model for ORN response [24], where it was shown that inclusion of inhibitory responses increases coding capacity of a distributed system of ORNs. Regarding decoding, recent works have pointed to the importance of a distributed response in inferring high-dimensional sparse signals [1, 25, 26]. In this work, we place particular importance on the impact of intensity variations that typify odor signals in natural environments, finding that in both static and fluctuating odor landscapes, adaptive sensing at the receptor level play a central role in the simulta-

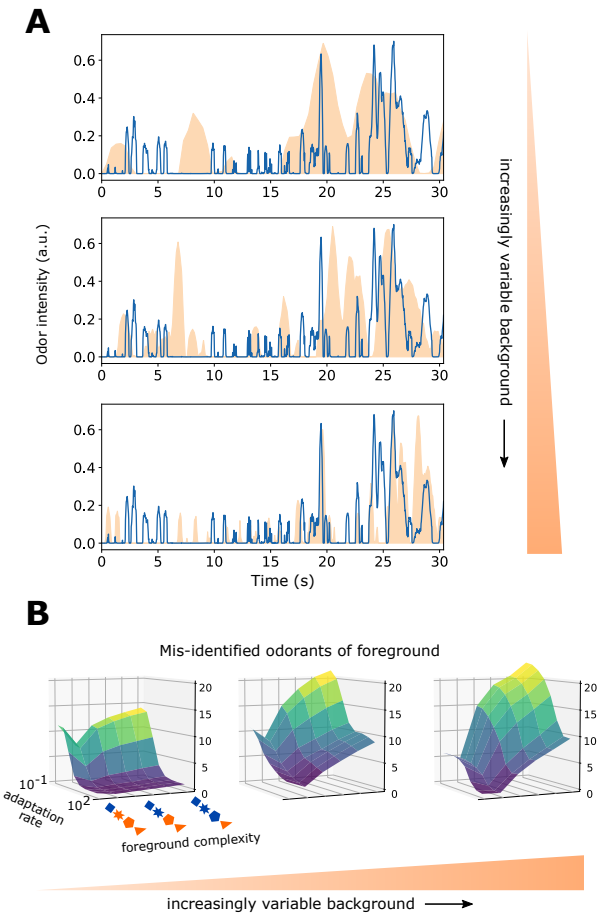

Figure 6: Dynamic adaptation maintains signal decoding fidelity amid fluctuating backgrounds at disparate timescales. **A** Traces of both odor signals, for three environments of increasingly faster background odor fluctuations. **B** Mis-identified odorants of foreground odor (blue trace in (A)), as a function of the relative complexity of the two odors and the adaptation rate.

neous decoding of odor intensity and odor identity.

a Maintaining a distributed response

We showed that for static odor signals, a broadly sensing but non-adaptive system can accurately estimate odor identities, though only in a limited window of concentration. In living systems, adaptation maintains information transfer by ensuring that the sensory system stays in a regime of maximum sensitivity [27]. In compressed sensing, the fidelity of signal decoding relies also on the combinatorics of the sensor response [18, 17, 19]. Indeed, it has been noted that *diffusivity* in sensing – here incorporated through the dispersity of binding constants – underlies effective compression of high-dimensional sparse signals into a limited receptor space. Still, the nonlinearity of the steady state receptor response, Eq. 1, can affect the distributions of ORN activity as odor concentration increases. Thus, in the context of combinatorial coding, the central benefit conferred by the Weber Law scaling is not merely preventing ORN activities from saturating, but their distributions from distorting.

Importantly, we find that the advantages of preserving combinatorial response carry over to more complex odor environments, where multiple odors must be discriminated. The ability to recognize weak odors over strong backgrounds is particularly relevant to olfaction in nature, where signal conflicts are pervasive. Absent Weber Law scaling, odor signals are mis-identified in the presence of strong backgrounds, producing accurate estimations only beyond a minimum intensity; this minimum itself increases with odor complexity. Further, the system is largely incapable of estimating both odors accurately – true discrimination – except in limited concentration windows. In principle, the adaptive system might also be susceptible to signal conflicts: mathematically, the activity distributions are invariant only in the limit that all odorants are of equal strength (Eq), so the large deviations of the weaker odorant concentrations from this mean value could lead to sensitive distortions in the distribution of ORN activities. Nonetheless, we find that odors at least as strong as the background can be identified irrespective of odor complexities. Likewise discrimination accuracy is more robust, preserved over sizable concentration windows.

b Simultaneous coding of intensity and identity

An important aspect of olfactory sensing is maintaining fidelity in encoding odor identity simultaneously with that of odor intensity [20]. Here we find that in some situations these aspects may decouple with variations in odor environment; often, though errors in one coincide with errors in the other. As mentioned, compressed sensing naturally conflates identity and intensity, decoding the exact strength of odor signal components while relying fundamentally on the requirement that most of components are zero. In this sense, combinatorial coding and compressed sensing decoding confronts the identity-intensity dilemma quite naturally, perhaps moreso than in sensory sys-

tems in which stimuli are parameterized continuously (e.g. by frequency), such as vision and audition. Still, evidence suggests that, at least in *Drosophila*, odor and intensity may be encoded in distinct regions in the mushroom body [21], so incorporating a more realistic neural model for decoding of sparse ORN response (such as in [26]) may find that these two aspects naturally segregate.

c Divisive normalization / timescales

TODO

d The timescales of adaptation mechanisms

We find that in naturalistic, intermittent odor environments, dynamic adaptation can promote active perception of sparse odors throughout whiffs. In particular, adaptation timescales around 100 ms are sufficient in maintaining ongoing refinements of perceived odor identity, and that these refinements confer robust and accurate odor identification within a short time (<500 ms) following whiff onset. We also find that sufficiently rapid adaptation aids odor intensity coding, although these gains are not as stark. Finally, dynamic adaptation can promote the accurate detection of fluctuating odors within background environments whose intensity variations are sufficiently slow.

Several studies have implicated the importance of ORN temporal dynamics in odor encoding [28, 29, 30, 31, 9, 32, 33, 34]. In mammalian olfaction, recent studies raise the possibility that the few most sensitive ORs are solely responsible for coding odor identity, a so-called "primacy code" [29]; such a representation is concentration invariant, as higher intensities would recruit the response of other, less sensitive receptors, but still retain this particular subset. While our results implicate *all* ORNs, not just the most sensitive, in faithful odor encoding [1], there are a few reasons to believe these two viewpoints are not inconsistent (aside from anatomical differences between the mammalian and insect olfactory periphery [35]). First, combinatorial coding applies to the identification of complex mixtures, not single odorants as tested in [29]. Second, while many odors may be encoded by distributed activity patterns in ORNs and corresponding glomeruli, some odors relevant for innate behaviors such as mating and feeding may contain their own dedicated pathways; these latter odors may rely on strong, specialized responses [34, 36]. The presence of broad and narrowly tuned olfactory receptors in *Drosophila* suggests that both combinatorial and primacy coding play distinct, complementary roles in naturalistic odor sensing.

Online Methods

a Stochastic odor-receptor binding model

We model an odor as an N-dimensional vector $\mathbf{s} = \langle s_1, ..., s_N \rangle$, where $s_i > 0$ are the concentrations of individual volatile molecules (odorants) comprising the odor. In addition, we assume that the odors are sparse in the space of odorants, so only K components of $\mathbf{s}$ are nonzero, where $K \ll N$. The olfactory sensory system is modeled as a collection of M distinct Or/Orco complexes, each of which can be bound with any one of the odorant molecules, and can be either active (firing) inactive (quiescent). We only consider competitive binding, so a complex is bound with one odorant at most. With N possible odorants, receptor a resides in one of $2N + 2$ possible states, $\{R_a$, R_a^*, R_a-s_i, R_a^*-$s_i\}$, indicating receptors that are unbound/inactive, unbound/active, inactive/bound to odorant i, and active/bound to odorant i, respectively. Unless otherwise indicated, we set $N = 100$, $K = 7$, and $M = 50$ throughout.

In the mean-field limit, the binding dynamics of these $2N+2$ states are described by the master equations:

$$\frac{d[R_a\text{-}s_i]}{dt} = k_{ia}^{+} s_i [R_a] - k_{ia}^{-} [R_a\text{-}s_i] \tag{3}$$

$$\frac{d[R_a^*\text{-}s_i]}{dt} = k_{ia}^{*+} s_i [R_a^*] - k_{ia}^{*-} [R_a^*\text{-}s_i], \tag{4}$$

when receptor R_a is either inactive (Eq. 3) or active (Eq. 4). Further, transitions between inactive and active states are described in the mean limit via:

$$\frac{d[R_a]}{dt} = w_a^{\mathrm{u}+} [R_a] - w_a^{\mathrm{u}-} [R_a^*] \tag{5}$$

$$\frac{d[R_a^*\text{-}s_i]}{dt} = w_{ia}^{\mathrm{b}+} [R_a\text{-}s_i] - w_{ia}^{\mathrm{b}-} [R_a^*\text{-}s_i], \tag{6}$$

when receptor R_a is either unbound (Eq. 5) or bound (Eq. 6). The corresponding disassociation constants in terms of the binding transition rates are:

$$K_{ia} = \frac{k_{ia}^{-}}{k_{ia}^{+}}$$

$$K_{ia}^{*} = \frac{k_{ia}^{*-}}{k_{ia}^{+*}} \tag{7}$$

Following [10], we assume that in steady state, the active firing state of an Or/Orco complex is energetically suppressed from the inactive state through corresponding Boltzmann factors:

$$\frac{[R_a^*]}{[R_a]} = \frac{w_a^{\mathrm{u}+}}{w_a^{\mathrm{u}-}} \equiv e^{-\epsilon_a} \tag{8}$$

$$\frac{[R_a^*\text{-}s_i]}{[R_a\text{-}s_i]} = \frac{w_{ia}^{\mathrm{b}+}}{w_{ia}^{\mathrm{b}-}} \equiv e^{-\epsilon_{ia}^{\mathrm{b}}}. \tag{9}$$

These energies are related through detailed balance, which we assume. Applying detailed balance to a given 4-cycle

$$R_a \rightarrow R_a^* \rightarrow R_a^*\text{-}s_i \rightarrow R_a\text{-}s_i \rightarrow R_a \tag{10}$$

gives

$$\frac{w_a^{\mathrm{u}+}}{w_a^{\mathrm{u}-}} \frac{k_{ia}^{*+}}{k_{ia}^{*-}} \frac{w_{ia}^{\mathrm{b}-}}{w_{ia}^{\mathrm{b}+}} \frac{k_{ia}^{-}}{k_{ia}^{+}} \equiv 1, \tag{11}$$

which, in conjunction with Eqs. 7, 8, and 9, gives

$$\epsilon_{ia}^{\mathrm{b}} = \epsilon_a + \ln\left[\frac{K_{ia}^*}{K_{ia}}\right]. \tag{12}$$

Assuming the binding dynamics are fast, then the probability that receptor a is bound by ligand i when inactive and active can be derived from Eqs. 3 and 4 as

$$p_{ia}^{\mathrm{b}} = \frac{s_i/K_{ia}}{1+\sum_j^N s_j/K_{ja}} \tag{13}$$

$$p_{ia}^{\mathrm{b},*} = \frac{s_i/K_{ia}^*}{1+\sum_j^N s_j/K_{ja}^*}. \tag{14}$$

The average activity A_a of complex a is the likelihood that the complex is active, unbound or unbound (equivalantly, the proportion of Or/Orco complexes in a given ORN that are active):

$$A_a = \frac{[R_a^*] + \sum_i^N [R_a^*\text{-}s_i]}{[R_a^*] + \sum_i^N [R_a^*\text{-}s_i] + [R_a] + \sum_i^N [R_a\text{-}s_i]}. \tag{15}$$

Using the master equations between active and inactive states Eq. 5 and 6, this activity obeys the master equation

$$\frac{dA_a}{dt} = w_a^+(1-A_a) + w_a^- A_a \tag{16}$$

with effective transition rates

$$w_a^+ = \sum_i^N p_{ia}^{\mathrm{b}} w_{ia}^{\mathrm{u}+} + p_a w_a^{\mathrm{u}} \tag{17}$$

and analogously for w_a^-. Setting Eq. 16 to zero gives the steady state average activity level of ORN a:

$$A_a = \left(1 + e^{\epsilon_a} \frac{1+\sum_i^N s_i/K_{ia}}{1+\sum_i^N s_i/K_{ia}^*}\right)^{-1}. \tag{1}$$

b Generation of binding matrices K_{ia}^*

K_{ia}^* matrices are generated by sampling at two stages. First, for each receptor complex a, the disassociation constants for ligand i were chosen uniformly: $K_{ia}^* \sim \mathcal{U}[\mu_a, \nu_a]$. Each of these bounds were themselves drawn from a hyperdistribution, also uniform, $\mu_a \sim \mathcal{U}[\mu_{a,\mathrm{L}}, \mu_{a,\mathrm{H}}]$ and $\nu_a \sim \mathcal{U}[\nu_{a,\mathrm{L}}, \nu_{a,\mathrm{H}}]$. The hyperdistribution determines receptor diversity (which receptors are broadly versus narrowly tuned), while the target distribution for a given a determines that receptor's particular tuning curve. K_{ia} matrix elements were set identically to 1e3 throughout.

c Compressed sensing decoding of ORN response

We decode ORN responses to infer odor signal identities using an abstraction intended to mimic the neural computations underlying odor identification in the *Drosophila* mushroom body. While we make no assumptions that the compressed sensing (CS) algorithm (or one like it) is being utilized in actuality, this framework nonetheless informs our understanding of how the neural representation of odor identity is maintained or lost when passed through a distributed ORN repertoire. In this sense, CS is somewhat of an upper bound on how well a real neural computation might perform in decompressing ORN responses.

We assume that ORN firing rates are linear in the Or/Orco complex activity; for simplicity we let this transform be the identity. Though subsequent neural circuitry, particularly from the glomeruli in the AL to the Kenyon cells in the MB further mix and scramble these responses, we focus here on the information transfer at the sensory periphery alone. In any case, as demonstrated previously [1], we expect that these neural computations would only improve the representation of neural identity, so we expect no negative ramifications for our findings.

CS addresses the problem of determining a sparse signal from a set of linear measurements, when the number of measurements is less than the signal di-

mension. Specifically, it is a solution to

$$\mathbf{y} = \mathbf{R}\mathbf{s}, \tag{18}$$

where $\mathbf{s} \in \mathbb{R}^N$ and $\mathbf{a} \in \mathbb{R}^M$ are vectors of signals and responses, respectively, and $\mathbf{R}$ is the measurement matrix. Since measurements are fewer than signal components, then $M < N$, whereby $\mathbf{R}$ is wide rectangular and so Eq. 18 cannot be simply inverted to produce $\mathbf{s}$. The idea of CS is to utilize the knowledge that $\mathbf{s}$ is sparse, i.e.g only K of its components, $K \ll N$ are nonzero. Both the measurements and sparsity are thus combined into a single constrained optimization routine:

$$\hat{s}_i = \text{argmin} \sum_i^N |s_i| \quad \text{such that } \mathbf{y} = \mathbf{R}\mathbf{s} \tag{19}$$

where $\hat{s}_i$ are the optimal estimates of the signal components and the sum, which is known as the L_1 norm of $\mathbf{s}$, is a natural metric of sparsity.

Importantly, the L_1 norm is a convex operation and the constraints are linear, so the optimization has a unique global minimum. To incorporate the nonlinear response of our encoding model into this linear framework, we assume that the responses are generated through the full nonlinear steady state response, Eq. 1, but that the measurement matrix needed for decoding uses a linear approximation of this transformation. Expanding Eq. 1 around $s_0 = s_i - \Delta s_i$ gives

$$A_a \approx A_{a,0} + \Delta A_a \tag{20}$$

$$\Delta A_a = \sum_i^N R_{ia}\big|_{s_0} \Delta s_i \tag{21}$$

$$A_{a,0} = \frac{\sum_1^N s_0/K_{ia}^*}{\sum_1^N s_0/K_{ia}^* + e^{\epsilon_a}} \tag{22}$$

$$R_{ia}\big|_{s_0} = \frac{e^{\epsilon_a}/K_{ia}^*}{(\sum_i^N s_0/K_{ia}^* + e^{\epsilon_a})^2}, \tag{23}$$

where we work in the approximation $K_{ia}^* \ll s_0 \ll K_{ia}$. We assume that the neural system has access to the linearized response, Eq. 23, but must infer the excess signals Δs_i from the excess activity ΔA_a. Corresponding to the CS framework, therefore, $\Delta\mathbf{A} \to \mathbf{y}$, $\Delta\mathbf{s} \to \mathbf{s}$, and $R_{ia}\big|_{s_0} \to \mathbf{R}$. We optimize the cost function in Eq. 19 using sequential least squares programming, implemented in Python through using the scientific package SciPy.

d Or/Orco energies of activation ϵ_a and enforcement of Weber's Law

Free energies are considered receptor-independent throughout, with the exception of dynamically adaptive system in a temporal odor environment (Figs. 5 and 6). To enforce Weber's Law, we assume the receptor activities feed back onto ϵ_a through the free energies. For the static case, adaptation is perfect, whereby Or/Orco activities are pegged to perfectly adapted values $\bar{A}_a$. Incorporating this into Eq. 1, and assuming $K_{ia}^* \ll s \ll K_{ia}$, gives

$$\bar{\epsilon}_a = \ln\left(\frac{1-\bar{A}_a}{\bar{A}_a}\right) + \ln\left(\sum_i^N \frac{s_i}{K_{ia}^*}\right). \tag{24}$$

Assuming that the excess signals are small, $\Delta s_i < s_0$, this gives

$$\epsilon_a \approx \ln(s_0) + \epsilon_{a,0}, \tag{25}$$

where $\epsilon_{a,0}$ are receptor-dependent constants. In the static case, we choose these constants such that ϵ_a in both adaptive and non-adaptive systems are equivalent, equal to ϵ_{L}, at a given low concentration, $s_{0,\text{L}}$. Below this concentration, we assume adaptation is not in effect, so $\epsilon_a = \epsilon_{\text{L}}$.

It is important to note that while the linearized gain Eq. 23 utilized by the decoding algorithm appears to rely on ϵ_a, by the above argument ϵ_a can in principle be determined by firing rates alone. That is, ϵ_a is inferred in time through integration of Eq. 2, which relies only on the current ORN activity.

e Odor signals

Odor signals $\mathbf{s}$ are N-dimensional vectors presumed sparse whereby only K components, s_k are nonzero, $K \ll N$. The magnitudes of the nonzero components s_k are denoted $s_0 + \Delta s_k$. Here, Δs_k is a random vector, while s_0 is both the center of linearization and, in the case of the adaptive system, the value dictating the strength of adaptive feedback $\epsilon_a \sim \ln\langle s_0\rangle$.

All the signal intensities are in arbitrary units, as they can be scaled to any range by a corresponding shift in the scales of K_{ia} and K_{ia}^*.

f Dynamic adaptation

Dynamic adaptation is enforced through

$$\frac{d\epsilon_a(t)}{dt} = \frac{1}{\tau_a}\left[A_a - \bar{A}_a\right]. \tag{2}$$

Figure	N	M	K	$\mu_{a,\mathrm{L}}$	$\mu_{a,\mathrm{H}}$	$\nu_{a,\mathrm{L}}$	$\nu_{a,\mathrm{H}}$	$\epsilon_{a,0}$	ϵ_{L}	ϵ_{H}	$s_{0,\mathrm{L}}$	s_k	$s_{k,\mathrm{F}}$
1c	200	40	6	$2 \cdot 10^{-4}$	10^{-3}	10^{-2}	1.0	5.4	5.4	10	-	$\mathcal{N}\left(\frac{s_0}{5}, \frac{s_0}{15}\right)$	–
2a	100	50	7	0.5	0.5	0.8	0.8	5.4	3.1	10	10^{-1}	$\mathcal{N}\left(\frac{s_0}{3}, \frac{s_0}{15}\right)$	–
2b	100	50	7	0.5	0.6	0.6	0.9	5.4	3.1	10	10^{-1}	$\mathcal{N}\left(\frac{s_0}{3}, \frac{s_0}{15}\right)$	—
2c	100	50	7	0.5	0.6	0.6	0.9	5.4	3.1	10	10^{-1}	$\mathcal{N}\left(\frac{s_0}{3}, \frac{s_0}{15}\right)$	–
4a-4h	100	50	7	0.5	0.6	0.6	0.9	5.4	3.1	10	10^{-1}	$\mathcal{N}\left(\frac{s_0}{3}, \frac{s_0}{15}\right)$	$\mathcal{N}(1, \frac{1}{5})$
5	100	50	7	0.5	0.6	0.6	0.9	–	–	–	10^{-2}	$\mathcal{N}\left(\frac{s_0}{3}, \frac{s_0}{9}\right)$	–
6	100	50	7	0.5	0.6	0.6	0.9	–	–	–	10^{-2}	$\mathcal{N}\left(\frac{s_0}{3}, \frac{s_0}{9}\right)$	–

Table 1: Parameters for simulations in all of the figures.

The perfectly adapted activity levels $\bar{A}_a$ are determined by evaluating Eq. 1 at a given odor intensity, $s_{0,\mathrm{L}}$, corresponding to a minimum stimulus at which adaptation takes effect. The decoding step is assumed instantaneous, so decoded odor identity $\hat{\mathbf{s}}$ is determined by the current value of ϵ_a (which, by virtue of Eq. 2, is determined by ORN activity a short time prior).

For the simulations with two fluctuating odors (Figs. 6), the traces shown correspond to the values of s_0 (in blue) and $s_{0,\mathrm{b}}$ (orange), where $s_{0,\mathrm{b}}$ is the baseline concentration of the background odor components, to which the excess signals $\Delta s_{k,\mathrm{b}}$ are added to set the individual odorant concentrations. We choose $\Delta s_{k,\mathrm{b}} \sim \mathcal{N}(s_{k,\mathrm{b}}/3, s_{k,\mathrm{b}}/9)$.

g Parameter values used in all figures

Parameter values for all of the plots are listed in Table 1.

References

[1] K. Krishnamurthy, A. M. Hermundstad, T. Mora, A. M. Walczak, and V. Balasubramanian, "Disorder and the neural representation of complex odors: smelling in the real world," *bioRxiv*, vol. doi:10.1101/160382, 2017.

[2] E. Hallem and J. Carlson, "Coding of odors by a receptor repertoire," *Cell*, vol. 125, no. 1, pp. 143–160, 2006.

[3] G. Wang, A. F. Carey, J. R. Carlson, and L. J. Zwiebel, "Molecular basis of odor coding in the malaria vector mosquito anopheles gambiae," *Proceedings of the National Academy of Sciences*, vol. 107, no. 9, pp. 4418–4423, 2010.

[4] R. I. Wilson, "Early olfactory processing in *Drosophila*: mechanisms and principles," *Annual Review of Neuroscience*, vol. 36, no. 1, pp. 217–241, 2013.

[5] S. Caron, V. Ruta, L. Abbott, and R. Axel, "Random convergence of olfactory inputs in the *Drosophila* mushroom body," *Nature*, vol. 497, no. 4774, pp. 113–117, 2013.

[6] H.-H. Lin, J. S.-Y. Lai, A.-L. Chin, Y.-C. Chen, and A.-S. Chiang, "A map of olfactory representation in the *Drosophila* mushroom body," *Cell*, vol. 128, no. 6, pp. 1205–1217, 2007.

[7] M. Heisenberg, "Mushroom body memoir: from maps to models," *Nature Reviews Neuroscience*, vol. 4, pp. 266–275, 2003.

[8] A. Celani, E. Villermaux, and M. Vergassola, "Odor landscapes in turbulent environments," *Phys. Rev. X*, vol. 4, p. 041015, Oct 2014.

[9] C. Martelli, J. R. Carlson, and T. Emonet, "Intensity invariant dynamics and odor-specific latencies in olfactory receptor neuron response," *Journal of Neuroscience*, vol. 33, no. 15, pp. 6285–6297, 2013.

[10] S. Gorur-Shandilya, M. Demir, J. Long, D. A. Clark, and T. Emonet, "Olfactory receptor neurons use gain control and complementary kinetics to encode intermittent odorant stimuli," *eLife*, vol. 6, p. e27670, jun 2017.

[11] L.-H. Cao, B.-Y. Jing, D. Yang, X. Zeng, Y. Shen, Y. Tu, and D.-G. Luo, "Distinct signaling of *Drosophila* chemoreceptors in olfactory sensory neurons," *Proceedings of the National Academy of Sciences*, vol. 113, no. 7, pp. E902–E911, 2016.

[12] J. Cafaro, "Multiple sites of adaptation lead to contrast encoding in the *Drosophila* olfactory system," *Physiological Reports*, vol. 4, no. 4, p. e12762, 2016.

[13] M. C. Larsson, A. I. Domingos, W. D. Jones, M. Chiappe, H. Amrein, and L. B. Vosshall, "Or83b encodes a broadly expressed odorant receptor essential for drosophila olfaction," *Neuron*, vol. 43, no. 5, pp. 703 – 714, 2004.

[14] H. Guo and D. P. Smith, "Odorant receptor desensitization in insects," *Journal of Experimental Neuroscience*, vol. 11, pp. 1–5, 2017.

[15] H. Guo, K. Kunwar, and D. Smith, "Odorant receptor sensitivity modulation in *Drosophila*," *The Journal of Neuroscience*, vol. 37, no. 39, pp. 9465–9473, 2017.

[16] S. R. Olsen, B. Vikas, and R. I. Wilson, "Divisive normalization in olfactory population codes," *Neuron*, vol. 66, pp. 287–299, 2010.

[17] D. Donoho, "Compressed sensing," *IEEE Transactions on Information Theory*, vol. 52, no. 4, pp. 1289–1306, 2006.

[18] E. Candes, J. Romberg, and T. Tao, "Robust uncertainy principles: Exact signal reconstruction from highly incomplete frequency information," *IEEE Transactions on Information Theory*, vol. 52, no. 2, pp. 489–509, 2006.

[19] S. Ganguli and H. Sompolinsky, "Compressed sensing, sparsity, and dimensionality in neuronal information processing and data analysis," *Annual Review of Neuroscience*, vol. 35, no. 1, pp. 485–508, 2012.

[20] M. Stopfer, V. Jayaraman, and G. Laurent, "Intensity versus identity coding in an olfactory system," *Neuron*, vol. 39, no. 6, pp. 991–1004, 2003.

[21] S. Xia and T. Tully, "Segregation of odor identity and intensity during odor discrimination in *Drosophila* mushroom body," *PLoS Biology*, vol. 5, no. 10, pp. 2398–2407, 2007.

[22] L. G., S. P., N. S., S. V., and T. Y., "The energy-speed-accuracy tradeoff in sensory adaptation," *Nature physics*, vol. 8, no. 5, pp. 422–428, 2012.

[23] Y. Tu, T. S. Shimizu, and H. C. Berg, "Modeling the chemotactic response of Escherichia coli to time-varying stimuli," *Proceedings of the National Academy of Sciences*, vol. 105, no. 39, pp. 14855–14860, 2008.

[24] L.-H. Cao, D. Yang, W. Wu, X. Zeng, B.-Y. Jing, M.-T. Li, S. Qin, C. Tang, Y. Tu, and D.-G. Luo, "Odor-evoked inhibition of olfactory sensory neurons drives olfactory perception in *Drosophila*," *Nature Communications*, vol. 8, no. 1, p. 1357, 2017.

[25] T. Tesileanu, S. Cocco, R. Monasson, and V. Balasubramanian, "Environmental adaptation of olfactory receptor distributions," *bioRxiv*, vol. doi:10.1101/255547, 2018.

[26] Y. Zhang and T. O. Sharpee, "A robust feedforward model of the olfactory system," *PLOS Computational Biology*, vol. 12, no. 4, pp. 1–15, 2016.

[27] I. Nemenman, "Information theory and adaptation," *arXiv*, vol. doi:[q-Bio]1011.5466, 2010.

[28] N. Gupta and M. Stopfer, "Insect olfactory coding and memory at multiple timescales," *Current Opinion in Neurobiology*, vol. 21, pp. 768–773, 2011.

[29] C. D. Wilson, G. O. Serrano, A. A. Koulakov, and D. Rinberg, "A primacy code for odor identity," *Nature Communications*, vol. 8, no. 1, p. 1477, 2017.

[30] S. Junek, E. Kludt, F. Wolf, and D. Schild, "Olfactory coding with patterns of response latencies," *Neuron*, vol. 67, no. 5, pp. 872 – 884, 2010.

[31] C.-Y. Su, C. Martelli, T. Emonet, and J. R. Carlson, "Temporal coding of odor mixtures in an olfactory receptor neuron," *Proceedings of the National Academy of Sciences*, vol. 108, no. 12, pp. 5075–5080, 2011.

[32] D. W. Wesson, R. M. Carey, J. V. Verhagen, and M. Wachowiak, "Rapid encoding and perception of novel odors in the rat," *PLoS Biology*, vol. 6, p. e82, 2008.

[33] H. Sanders, B. E. Kolterman, R. Shusterman, D. Rinberg, A. Koulakov, and J. Lisman, "A network that performs brute-force conversion of a temporal sequence to a spatial pattern: relevance to odor recognition," *Frontiers in Computational Neuroscience*, vol. 8, p. 108, 2014.

[34] Y. Seki, D. H. K.M., R. J., D. Wicher, S. Sachse, and B. S. Hansson, "Olfactory coding from the periphery to higher brain centers in the drosophila brain," *BMC Biology*, vol. 15, p. 56, 2017.

[35] B. S. Hansson and M. C. Stensmyr, "Evolution of insect olfaction," *Neuron*, vol. 72, no. 5, pp. 698 – 711, 2011.

[36] M. N. Andersson, C. Lfstedt, and R. D. Newcomb, "Insect olfaction and the evolution of receptor tuning," *Frontiers in Ecology and Evolution*, vol. 3, p. 53, 2015.